NASA Technical Memorandum 87604

THE EFFECT OF RESIN TOUGHNESS AND MODULUS ON COMPRESSIVE FAILURE MODES OF QUASI-ISOTROPIC GRAPHITE/EPOXY LAMINATES

MOHSEN M. SOHI, H. THOMAS HAHN, AND JERRY G. WILLIAMS

MARCH 1986

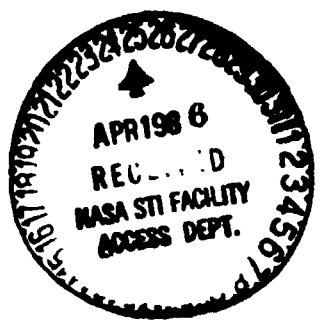

National Aeronautics and Space Administration

Langley Research Center
Hampton, Virginia 23665

THE EFFECT OF RESIN TOUGHNESS AND MODULUS ON COMPRESSIVE FAILURE MODES OF QUASI-ISOTROPIC GRAPHITE/EPOXY LAMINATES

by

Mohsen M. Sohi and H. Thomas Hahn
Washington University
St. Louis, MO 63130

and

Jerry G. Williams
NASA Langley Research Center
Hampton, VA 23665-5225

ABSTRACT

Compressive failure mechanisms in quasi-isotropic graphite/epoxy laminates were characterized for both unnotched and notched specimens and also following damage by impact. Two types of fibers (Thornel 300 and 700) and four resin systems (Narmco 5208, American Cyanamid BP907, and Union Carbide 4901/MDA and 4901/mPDA) were studied. The widely used T300/5208 served as the baseline composite system. For all material combinations, failure of unnotched specimens was initiated by kinking of fibers in the 0-degree plies. A major difference was observed, however, in the mode of failure propagation after the 0-degree ply failure. In laminates made with Narmco 5208 resin, the 0-degree ply failure was immediate followed by delamination and catastrophic failure of the specimen. In BP907 resin the fiber kinking was well contained without delamination, and still allowed further increase in load. The remaining two resins lay between BP907 and Narmco 5208 in their resistance to delamination. The strength of quasi-isotropic laminates in general increased with increasing resin tensile modulus. The laminates made with Thornel 700 fibers exhibited slightly lower compressive strengths than did the laminates made with Thornel 300 fibers. The notch sensitivity as measured by the hole strength was lowest for the BP907 resin and highest for the 5208 resin. For the materials studied,

however, the type of fiber had no effect on the notch sensitivity. The area of impact damage was smallest for the BP907 resin. The 4901 resins were comparable to the 5208 resin in their impact resistance. Of the two fiber types, the T700 fiber consistently gave smaller damage area. The strength reduction after impact could be explained from the impact damage area and the unnotched strength.

INTRODUCTION

One of the drawbacks in the application of the current graphite/epoxy composites in structures is their high susceptibility to low velocity impact damage [1-5]. Due to the brittleness of the matrix resins used, low velocity impact often results in matrix cracking, delamination and fiber fracture. Under compressive loading the damage caused by impact leads to premature failure and results in an unacceptable loss of strength.

Recent studies have indicated that the extent of impact damage can be reduced by using tougher resins [3-6]. However, the use of tougher resins may result in the reduction of compressive strength because toughness is frequently obtained at the sacrifice of stiffness. Therefore, a proper compromise must be maintained between toughness and stiffness to improve impact resistance without risking a compressive failure.

The effect of resin properties on compressive behavior of unidirectional composites was studied in References 7, 8 and 9. It was found that the compressive strength increased and the mode of fiber failure changed from buckling to kinking, as the resin tensile modulus increased.

In the present paper, the same material systems used in References 7 and 8 were used to study the effect of resin modulus and toughness on compressive failure of quasi-isotropic laminates with and without a hole and after damage by impact. Notch sensitivity was measured using holes of different diameters. Impact resistance was characterized by the impact damage area and post-impact strength retention.

MATERIALS

The fibers used were Thornel 300 (T300) and Thornel 700 (T700). These

two fibers have approximately the same Young's modulus (about 230 GPa). The T700 fiber, however, has a higher tensile failure strain and a smaller diameter. These two fibers were combined with Narmco 5208, American Cyanamid BP907, and Union Carbide 4901/MDA and 4901/mPDA to provide seven different material systems. All laminates were fabricated according to the manufacturers' suggested cure cycles at the NASA Langley Research Center. The Narmco 5208 resin, which was the baseline resin system, has the lowest tensile failure strain among all the resins used. The BP907 resin has the lowest tensile modulus and the Union Carbide 4901/mPDA resin the highest tensile modulus. Mechanical properties of the constituent materials are presented in Table 1. The BP907 resin is known to be tougher than the 5208 resin [5]; however, the toughness of 4901 resins is not known.

SPECIMEN PREPARATION AND TESTING

Unnotched Specimens

Ultimate compressive strength and failure modes were studied using 24-ply laminates with a stacking sequence of $[45/0/-45/90]_{3S}$. The laminates were cut and tabbed into a geometry appropriate for an IITRI (Illinois Institute of Technology Research Institute) compression fixture. Testing was done on an Instron testing machine at a crosshead speed of 1 mm/min. During loading, specimens were monitored through a stereo microscope at magnifications up to 100X for indications of failure. Some specimens were tested in a loading-unloading mode; that is, the specimen was loaded to a certain level and then unloaded. Upon unloading the specimen was removed and examined for failure using an optical microscope at magnifications up to 500X. The stress-strain response for each material was determined using a

strain gage bonded to one of the lateral faces of two specimens in each material system.

Specimens With Open Hole and Impact Damage

Two types of specimens were used to study the notch sensitivity. One group of specimens were $[45/0/-45/90]_{3S}$ laminate coupons 25 mm wide by 44.5 mm long with a center hole ranging from 3.18 to 9.54 mm in diameter. A special plate fixture was used to grip the specimen at the ends with slight side pressure. Axial load was introduced to the two edges bearing on the plates.

The other group of specimens were $[45/0/-45/90]_{6S}$ laminates. They were 127 mm wide by 254 mm long and had a 25 or 50-mm-diameter center hole. These specimens were tested according to the procedure described in [5].

The impact specimens were also $[45/0/-45/90]_{6S}$ laminates 127 mm wide by 254 mm long. Impact damage was inflicted by striking the specimen with a 1.27-cm-diameter aluminum sphere propelled by compressed air. Two impact energies were employed: 17 J and 34.4 J which corresponded to projectile speeds of approximately 110 m/s and 154 m/s, respectively. Following the impact, the specimen was inspected visually and ultrasonically to determine the extent of damage. Details of the test procedure are reported in [3].

RESULTS AND DISCUSSION

Unnotched Specimens

Failure Modes - Compressive failure of unnotched quasi-isotropic specimens was usually catastrophic. Occasional arrest of partially failed specimens was possible only by the loading-unloading procedure described previously. Failure was usually initiated in the vicinity of the tab ends,

although subsequent failure was spread over the entire gauge length.

Examinations of partially failed specimens suggest that compressive failure of quasi-isotropic laminates is triggered by the kinking of fibers in the 0-degree plies. This is followed by delamination and subsequent buckling of sublaminates.

Figure 1 shows a partially failed T300/BP907 specimen which was loaded to 81% of the average ultimate compressive strength (UCS). Figure 1 (a) is the failure of a 0-degree ply as seen on an edge of the specimen. Propagation of the failure in the plane of the 0-degree ply is seen in Figure 1 (b), where the top nine plies were ground away to expose the failed 0-degree ply. The figures clearly show kinking of fibers in the 0-degree ply. No delamination is present and the adjacent off-axis plies are intact. It is therefore concluded that kinking of the 0-degree fibers precedes any other failure event. In this specimen, only the 0-degree ply shown in the figure had failed by kinking, and all the other 0-degree plies were intact.

Figure 2 shows a similar partial failure of a T700/4901/MDA specimen loaded to 93% UCS. The 0-degree ply shown in Figure 2(b) has had the outer plies removed by grinding and indicates fiber kinking initiated at the free edge since failure exists only in this region.

Partial failures in the other laminates are shown in Figure 3. All laminates except T700/4901/mPDA have only one 0-degree ply failure.

The maximum prestress levels indicated in the figure, which were applied before the detection of kinking, are very close to the respective ultimate compressive strengths except for the laminates with the BP 907 resin. The BP 907 resin is the toughest of the resins used in the present study, and hence appears to be better able than the other resins to resist

delamination following fiber kinking. Yet, this resin allows fiber kinking to occur at lower strains than the other resins do. The same trend was observed in unidirectional composites [7].

The T700/4901/mPDA laminate was loaded to the highest relative prestress level and shows failure in two 0-degree plies. Therefore, the sequential failure of 0-degree plies may occur prior to ultimate failure of the laminate. Fiber kinking in a 0-degree ply is progressive, as shown in Figure 1 and, therefore, one might expect multiple failure initiation sites.

Arrest of fiber kinking before catastrophic propagation was most difficult for the T300/5208 laminate. Failure was quite sudden with extensive delamination after ultimate failure. Therefore, this laminate was judged to be the most brittle.

Although the laminates differ in the progression of damage, failure initiation in all seven composite systems is believed to be governed by the same mechanism; namely, the fiber kinking in 0-degree plies. The following is the concluded sequence of events that leads to the final failure of quasi-isotropic graphite/epoxy laminates:

1. As the compressive load increases, fiber kinking occurs in a 0-degree ply at an edge and propagates inward. The rotation of broken fiber segments in a kink band is both in and out of the plane of the 0-degree ply. The fiber kinking is of the same type as observed in unidirectional graphite/epoxy composites described in Reference 7.
2. Failure of a 0-degree ply not only transfers the load to other 0-degree plies, but also results in load eccentricity since the specimen loses stiffness on the side with the failed ply. This enhances a sequential rather than random failure of the remaining 0-degree plies starting with

the one closest to the failed ply and propagating outward, Figure 3 (e).

3. A 0-degree ply with fiber kinking may move relative to the neighboring angle plies. This brings about delamination between the failed 0-degree ply and the angle plies.

4. After delamination, the sublaminates are more susceptible to buckling than the original laminate because of thinner thicknesses. The global buckling of sublaminates leads to final failure as shown in Figure 4.

Compressive Behavior - Typical stress-strain curves for the different laminates are shown in Figure 5. All the stress-strain curves exhibited strain softening which suggests the specimens did not experience global buckling. The reason is that the lateral surface on which the strain gage was to be bonded was chosen randomly and it is highly unlikely that all the gages would have been placed on the compression side by mere coincidence. The absence of global buckling was furthermore confirmed by using back-to-back strain gages on both sides of a T700/BP907 specimen. Figure 6 shows the strain outputs in which no strain reversal is observed.

The critical buckling stress, including the effect of composite transverse shear modulus, was calculated for a T300/5208 laminate (cf. Appendix). The same stacking sequence as in the unnotched specimens was assumed. Since no specimen-tab debonding was observed in the experiments, a column length equal to the specimen gage length was used in the calculations. In order to get a conservative estimate of the buckling stress, the column ends were assumed to be simply supported.

Including the effect of induced transverse shear forces was seen to reduce the critical buckling stresses by 52 % (see Appendix). The resulting required stress of 1774 MPa to cause global buckling was, however, much

higher than the 726 MPa obtained as the average failure stress. The other six laminates are expected to behave similarly since their mechanical properties are similar to those of the T300/5208 laminate. Therefore, it is concluded that the quasi-isotropic laminates tested failed in compression long before the critical buckling stress was reached.

Some of the specimens were loaded well into the nonlinear region and then unloaded. The stress-strain relation during unloading was almost the same as during loading, Figure 7. Thus, the nonlinearity is not believed to have been caused by damage. In fact, the corresponding unidirectional composites also showed similar nonlinear behavior [7].

Although fiber kinking occurred in 0-degree plies before ultimate failure, as discussed earlier, it could not be detected on the stress-strain curves. No abrupt change in stress or strain was observed up to final failure.

Compressive properties of all seven quasi-isotropic laminates are listed in Table 2. In general, the quasi-isotropic strengths have a lower scatter band than the unidirectional strengths reported in References 7 and 8. Even the T300/5208 composite, which showed considerable scatter in unidirectional strength, is fairly consistent in quasi-isotropic strength. A smaller scatter in strength indicates less sensitivity to defects. Although the initial fiber kinking acts as a defect after its inception, it is less critical to ultimate failure of quasi-isotropic laminates than that of unidirectional laminates. This conclusion is borne out by the ease with which fiber kinking can be monitored in quasi-isotropic laminates.

The average compressive strengths of quasi-isotropic laminates are plotted against the resin tensile moduli in Figure 8. As for unidirectional

composites [7], the compressive strength increases with increasing resin modulus.

Although in tension the T700 fiber is stronger than the T300 fiber the corresponding laminates show the opposite trend in compression. Both failure stresses and failure strains for T700 laminates are lower than for T300 laminates probably because of the smaller diameter of the T700 fiber. According to the nonlinear microbuckling model presented in Reference 7, the compressive strength of a 0-degree ply is inversely related to the initial fiber curvature. Since a larger diameter fiber is likely to have a smaller initial curvature, compressiv strength of composites will increase with fiber diameter.

The T300/5208 laminate shows the highest compressive failure strain despite the fact that the 5208 resin has the lowest tensile failure strain of all four resins used. The failure strains of quasi-isotropic laminates are compared with those of unidirectional laminates of the same material systems [7] in Figure 9. The quasi-isotropic laminates are seen to have considerably higher failure strains than the corresponding unidirectional laminates. This is due to a better lateral support provided to the 0-degree plies by adjacent off-axis plies in quasi-isotropic laminates. The in-plane kinking in the quasi-isotropic laminate is influenced by the higher stiffness of off-axis plies normal to the loading. The out-of-plane kinking also is re arded by the off-axis fibers bridging over the kink band.

Specimens With Holes

The failure of specimens with a circular hole was also initiated by fiber kinking in the 0-degree plies, as reported in References 4 and 10.

Similar to the findings of Reference 4, the initial failure started at the hole boundary and propogated towards the specimen edges.

The sequence of failure events suggested in References 4 and 10 did not include any comparison between laminates with brittle resin and with soft resin. As in the unnotched laminates, the mode of failure propagation following the initial fiber kinking changed with the ductility of the resin used. In the T300/5208 laminate, delamination immediately followed the initiation of a kink band, Figure 10. Two outer 0-degree plies failed in the form of kinking, causing local delamination of the outside 45-degree ply from the adjacent 0-degree ply. Upon further increase in load, the failure band propagated along the specimen width. The fiber kinking in the 0-degree plies, coupled with the seperation of 45-degree plies, induced further delamination. Figure 10 (b) shows the polished lateral surface of the same specimen as shown in Figure 10 (a). The outer 45-degree ply was ground away to expose the fiber kinking in the 0-degree ply. Intraply cracking is also observed in a 45-degree and a 90-degree ply, Figure 10.

A combination of fiber kinking in 0-degree plies and delamination was also observed in laminates made with 4901/MDA and 4901/mPDA resins. Similar to the T300/5208 laminate, failure was initiated in the outer 0-degree plies, Figure 11. In these laminates, however, the kink band had propagated farther through the width of the ply when the test was stopped. It was therefore difficult to assess whether these laminates were any more tolerant of the initial damage than was the T300/5208 laminate.

In laminates made with the BP907 resin, the kink band propagated some distance away from the hole before causing any delamination. Figure 12 shows partial damage in a T700/BP907 specimen. Although all the 0-degree

plies have failed, no delamination is present. Since the kink band shown in Figure 12 traveled more than one-fourth of the net specimen width on each side of the hole, it can be deduced that delamination was delayed up to an advanced stage of failure. Therefore, laminates made with the BP907 resin fail when most 0-degree plies fail completely accompanied by very little delamination.

Notched strengths of 25 mm wide specimens were analyzed according to the point-stress failure criterion of Whitney and Nuismer [11]. For an infinite quasi-isotropic plate with a hole of radius R, the point-stress failure criterion predicts the notched strength σ_N^∞ to be

$$\sigma_N^\infty/\sigma_o = 2 \; / \; (\; 2 + \zeta^2 + 3\zeta^4) \tag{1}$$

where σ_o is the unnotched strength and

$$\zeta = R/(R + d_o) \tag{2}$$

Here, d_o defines the distance from the hole boundary to a point where the normal stress in the loading direction reaches σ_o at final failure.

The experimental notched strength σ_N obtained from a specimen of finite width can be converted to σ_N^∞ using the finite width correction factor Y:

$$\sigma_N^\infty = Y \; \sigma_N \tag{3}$$

$$Y = \frac{2 + (1 - 2R/W)^3}{3(1 - 2R/W)} \tag{4}$$

where W is the specimen width.

Equations (1) - (4) were used together with the unnotched strengths (given in Table 2) and the experimental notched strengths to calculate the

average value of d_o for each composite system tested, and the results are shown in Figure 13. As can be seen from Equations (1) and (2), a higher d_o indicates less notch sensitvity, i.e., less reduction in the normalized notched strength σ_N^∞/σ_o with increasing hole size.

As expected, T300/BP907 and T700/BP907 laminates show the least notch sensitivity while the T300/5208 shows the most. The two curing agents MDA and mPDA yield almost the same notch sensitivity. Also, the notch sensitivity is more dependent on the matrix material type than on the fiber.

With d_o experimentally determined, the change of strength ratio σ_N/σ_o with normalized hole diameter 2R/W as calculated by Equations 1 through 4 is shown together with the experimental data for each laminate in Figures 14 and 15. The experimental data for $[45/0/-45/90]_{6S}$ specimens 127 mm wide and 254 mm long are shown in Figures 16 and 17. Also shown in the latter figures are the predictions for the large specimens using the d_o values obtained from the small specimens. The agreement between the experimental results and the predictions is quite reasonable.

Impact Damage

The extent of damage due to impact is shown in Figure 18, where the damage areas measured on ultrasonic C-scan records are plotted against the impact energies. The figure also includes the data for other composite systems reported in Reference 5. Whereas two different impact energies were used for the laminates made with 4901/mPDA resin, only the lower impact energy was used for the laminates made with 4901/MDA resin. Of all resins shown, BP907 gives the best impact resistance.

The T700 fiber shows better impact resistance than the T300 fiber. During impact large local deformation gradients occur which cause high

tension stresses to develop on the back surface. The T700 fiber with its higher strain capability can sustain higher back surface tension strains prior to failure than the lower strain capability T300 fiber.

The 4901 resin yields laminates which, in impact damage size, rank somewhere between the BP907 laminates and the T300/5208 laminate, the former being the most resistant to impact.

The failure strength for specimens loaded in compression following impact damage at selected impact energies is presented in Figure 19. Laminates constructed using BP907 resin and the higher strain T700 fiber recorded a higher failure strength than did BP907 laminates with T300 fiber.

CONCLUSIONS

Compressive behavior of quasi-isotropic graphite/epoxy laminates was studied using two different fibers (T300 and T700) and four different resins (5208, BP907, 4901/MDA, and 4901/mPDA). The IITRI compression fixture was used to study the unnotched behavior while holes of varying diameters were used to study the notch sensitivity. The effect of low velocity impact on structural integrity was characterized in terms of damage area and the strength retention after impact. The following conclusions are drawn from the present study.

1. Failure of the quasi-isotropic laminates under compression was initiated by fiber kinking in the 0-degree plies. The fiber kinking started at an edge and grew inward.

2. The fiber kinking was initially contained in the tough BP907 resin; however, it immediately led to delamination and ultimate failure in the brittle 5208 resin. Based on the failure modes, the 4901 resin cured with

MDA or mPDA was judged to be between BP907 and 5208 resins in its toughness.

3. Failure strains for the quasi-isotropic laminates were higher than those for the corresponding unidirectional laminates because the quasi-isotropic laminates could locally contain the fiber kinking better than the unidirectional laminates.

4. The compressive strength increased with the resin tensile modulus.

5. Failure initiation in the specimens with a hole was also fiber kinking in the 0-degree plies. Fiber kinking occurred at the point of maximium compressive stress and grew inward. Growth of the kink band was most gradual in the BP907 resin and the least stable in the 5208 resin. The notch sensitivity was the lowest for the laminates made with the BP907 resin and the highest for those made with the 5208 resin. The fiber type (T300 versus T700) did not seem to significantly affect the notch sensitivity. Previous investigations (Reference 4) have shown higher strain fibers (AS4 versus T300) to improve open-hole compression strength. The smaller diameter of the T700 fiber (Table 1) may be a factor which counteracts the improvement expected from a higher strain fiber.

6. The BP907 resin allowed the least impact damage while the 4901 resins were comparable to the 5208 resin. The T700 fiber resulted in better resistance to impact damage than the T300 fiber probably due to its higher strain capability. The T700/BP907 laminate showed the highest residual strength, followed by the T300/BP907 laminate. The remaining laminates were comparable to one another in their residual strengths.

REFERENCES

1. Rhodes, M.D., J.G. Williams, and J.H. Starnes: Effect of Low Velocity Impact Damage on the Compressive Strength of Graphite/Epoxy Hat-Stiffened Panels. NASA TN D-8411, 1977.

2. Starnes, J.H., Jr., M.D. Rhodes, and J.G. Williams: Effect of Impact Damage and Holes on the Compressive Strength of a Graphite/Epoxy Laminate. Nondestructive Evaluation and Flaw Criticality for Composite Materials, ASTM STP 696, 1979, pp. 145-171.

3. Williams, J.G. and M.D. Rhodes: Effect of Resin on Impact Damage Tolerance of Graphite/Epoxy Laminates. Composite Materials: Testing and Design, ASTM STP 787, I.M. Daniel, Ed., ASTM, 1982, pp. 450-480.

4. Williams, J.C.: Effect of Impact Damage and Open Holes on the Compression Strength of Tough Resin/High Strain Fiber Laminates. NASA TM-85756, February 1984.

5. Williams, J.G., T.K. O'Brien and A.J. Chapman, III: Comparison of Toughened Composite Laminates Using NASA Standard Damage Tolerance Tests. NASA CP-2321, ACEE Composite Structures Technology Conference, Seattle, Washington, August 1984.

6. Palmer, R.J.: Investigation of the Effect of Resin Materials on Impact Damage to Graphite/Epoxy Composites. NASA CR 165677, March 1981.

7. Hahn, H.T., and J.G. Williams: Compression Failure Mechanisms in Unidirectional Composites. NASA TM 85834, August 1984.

8. Sohi, M.M.: Compressive Behavior of Graphite/Epoxy composites. M.S. Thesis, Washington University, St. Louis, Mo., December 1984.

9. Hahn, H.T.: Effect of Constituent Properties on Compressive Failure Mechanisms. Tough Composite Materials Workshop, NASA CP 2334. May 1983.

10. Rhodes, M.D., M.M. Mikulas, Jr., and P.E. McGowan: Effects of Orthotropy and Width on the Compression Strength of Graphite-Epoxy Panels with Holes. AIAA Journal, Vol. 22, No. 9, September 1984, pp. 1283-1292.

11. Whitney, J.M., and R.J. Nuismer: Stress Fracture Criteria for Laminated Composites Containing Stress Concentrations. J. of Composite Materials, 8, 1974, pp. 253-265.

12. Timoshenko, S.P. and J.M Gere: Theory of Elastic Stability. New York, McGraw Hill Book Co., Inc., 1961, p. 132.

13. Hahn, H.T. and R.Y. Kim: Swelling of Composite Laminates. Advanced Composite Materials--Environmental Effects, ASTM STP 658, 1978, pp. 98-120.

APPENDIX : CALCULATION OF THE CRITICAL BUCKLING STRESS

1. Notation

Figure 20 shows the coordinate system, the laminate orientation, and the stress notation used.

2. Buckling Formula

If the transverse shearing forces induced by deformation are taken into account, the critical buckling force in a column is given by [12]:

$$P_{cr} = \frac{P_e}{1 + (n\ P_e) / (A\ G_{13})} \qquad \text{(A-1)}$$

where

$$P_e = (\pi / L_e)^2\ D_{11} \qquad \text{(A-2)}$$

and

D_{11} = flexural stiffness

L_e = effective length (= L for simply supported ends)

A = cross sectional area

n = a numerical factor depending on the cross section (=1.2 for rectangular shape)

G_{13} = transverse shear modulus

3. Unidirectional T300/5208 Properties Used in The Calculations

E_1 = 131.0 GPa $\qquad \nu_{21}$ = 0.380

E_2 = 13.0 GPa $\qquad \nu_{12}$ = 0.038

$E_3 = E_2 \qquad \nu_{13} = \nu_{12}$

G_{12} = 6.4 GPa $\qquad \nu_{23}$ = 0.492

$G_{31} = G_{12} \qquad \nu_{32} = \nu_{23}$

G_{23} = 3.02 GPa (via the modified rule-of-mixtures assuming V_f = 0.6, E_m = 4.0 GPa, ν_m = 0.35, and G_{f2} = 5.9 GPa)

4. The On-Axis Compliance Matrix

$$[S] = \begin{bmatrix} 1/E_1 & -\nu_{12}/E_2 & -\nu_{13}/E_3 & 0 & 0 & 0 \\ -\nu_{21}/E_1 & 1/E_2 & -\nu_{23}/E_3 & 0 & 0 & 0 \\ -\nu_{31}/E_1 & -\nu_{32}/E_2 & 1/E_3 & 0 & 0 & 0 \\ 0 & 0 & 0 & 1/G_{23} & 0 & 0 \\ 0 & 0 & 0 & 0 & 1/G_{31} & 0 \\ 0 & 0 & 0 & 0 & 0 & 1/G_{12} \end{bmatrix} \quad \text{(A-3)}$$

substituting the unidirectional properties,

$$[S] = \begin{bmatrix} 0.00763 & -0.00290 & -0.00290 & 0 & 0 & 0 \\ -0.00290 & 0.07692 & -0.03785 & 0 & 0 & 0 \\ -0.00290 & -0.03785 & 0.07692 & 0 & 0 & 0 \\ 0 & 0 & 0 & 0.33069 & 0 & 0 \\ 0 & 0 & 0 & 0 & 0.15625 & 0 \\ 0 & 0 & 0 & 0 & 0 & 0.15625 \end{bmatrix} \quad \text{(A-4)}$$

5. On-Axis Stiffness Matrix

$$[C] = \begin{bmatrix} 138.9 & 10.3 & 10.3 & 0 & 0 & 0 \\ 10.3 & 17.9 & 9.2 & 0 & 0 & 0 \\ 10.3 & 9.2 & 17.9 & 0 & 0 & 0 \\ 0 & 0 & 0 & 3.02 & 0 & 0 \\ 0 & 0 & 0 & 0 & 6.4 & 0 \\ 0 & 0 & 0 & 0 & 0 & 6.4 \end{bmatrix} \quad \text{(A-5)}$$

6. Calculation of D_{11}

D_{11} was calculated using the following formula

$$D_{ij} = \int_{-h/2}^{+h/2} C_{ij}\, z^2 \, dz \qquad \text{(A-6)}$$

where z is the coordinate in the thickness direction. Assuming a $[45/0/-45/90]_{3S}$ stacking sequence and a ply thickness of 0.14 mm yields

$$D_{11} = 203500 \text{ N mm}$$

7. Calculation of G_{13}

Using contracted notation, stress-strain relation of a constituent ply can be written as

$$\sigma_i = C_{ij}\, \varepsilon_j + C_{iA}\, \varepsilon_A \qquad \text{(A-7)}$$

$$\sigma_A = C_{Aj}\, \varepsilon_j + C_{AB}\, \varepsilon_B \qquad \text{(A-8)}$$

where i, j = 1, 2, 6 are associated with the in-plane coordinates and A, B = 3, 4, 5 with the out-of-plane coordinates. According to the classical laminated plate theory, σ_A are assumed to be constant throughout the thickness. If the total strains ε_i are displayed as $\varepsilon_i = \varepsilon_i^0 + kz$, then one can show that [13],

$$\bar{\varepsilon}_A = \overline{C_{AB}^{-1}}\ \sigma_B + \overline{C_{AB}^{-1}\, C_{Bj}}\ \varepsilon_j^0 - \overline{C_{AB}^{-1}\, C_{Bj}}\ z\, k_j \qquad \text{(A-9)}$$

where ε_i^0 and k_j are the in-plane strains and curvatures, respectively. An overbar stands for average through the thickness h, i.e.

$$\overline{(\ \ )} = \frac{1}{h} \int_{-h/2}^{h/2} (\ \ )\, dz$$

Assuming $\sigma_3 = \sigma_4 = \varepsilon_j = k_j = 0$, Equation (A-9) yields

$$\bar{\varepsilon}_5 = \overline{C_{55}^{-1}}\ \sigma_5 \qquad \text{(A-10)}$$

where C_{55}^{-1} is the element in the fifth row and fifth column of $[C_{ij}]^{-1}$. The transverse shear modulus is then given by

$$G_{13} = \frac{1}{\overline{C_{55}}^{-1}} \qquad \text{(A-11)}.$$

Using the on-axis stiffness matrix given in (A-5), a $[45/0/-45/90]_{3S}$ stacking sequence, and a ply thickness of 0.14 mm results in

$$G_{13} = 4.1 \text{ GPa}$$

8. The Critical Buckling Stress

Substituting $D_{11} = 203500$ N mm, $G_{13} = 4.1$ GPa, $n = 1.2$, $A = 21.3$ mm^2, and $L_e = 12.7$ mm in (A-2) and (A-1), gives

$$P_{cr} = 37828 \text{ N}$$

or $$\sigma_{cr} = P_{cr}/A = 1774 \text{ MPa}.$$

Table 1: Properties of the Constituent Materials.

Material	Diameter (10^{-6} m)	Modulus[1] (GPa)	Failure[1] Stress (MPa)	Failure[1] Strain (%)
T300	7.0	230.00	3310.0	1.4
T700	5.1	238.00	4550.0	1.9
BP907	-	3.10	89.5	4.8
5208	-	4.00	57.2	1.8
4901/ MDA	-	4.62	103.4	4.0
4901/ mPDA	-	5.46	115.1	2.4

[1]: In Tension

TABLE 2: Properties of the Composite Laminates

COMPOSITE	FIBER WEIGHT CONTENT (%)	FAILURE STRESS[a] AVERAGE (MPa)	C.V. (%)	FAILURE[b] STRAIN (%)	MODULUS[b] (GPa)
T300/5208	57	726	3.4	2.05	46.5
T300/BP907	58	529	5.3	1.64	43.4
T300/490 /MDA	67	734	6.6	1.51	58.3
T300/4901 mPDA	69	774	3.4	1.57	64.3
T700/BP907	59	526	2.8	1.31	45.5
T700/4901 /MDA	65	682	8.8	1.25	59.9
T700/4901 /mPDA	65	709	4.6	1.34	58.7

[a] Eight specimens tested for T300/ and T700/BP907.
Ten specimens tested for the other laminates.

[b] Two specimens tested.

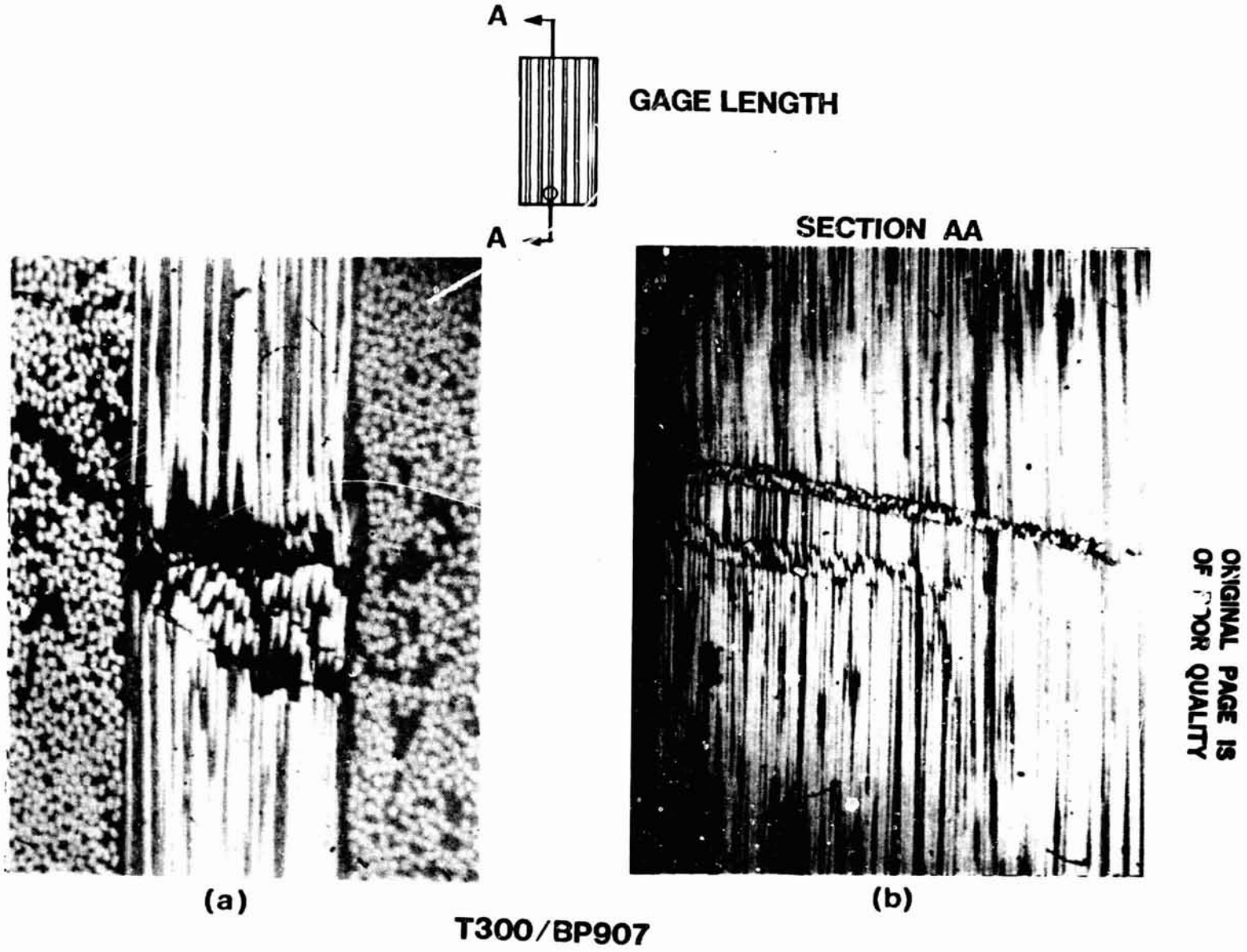

Figure 1. Partial failure in a T300/BP907 specimen loaded to 81% of the average ultimate compressive strength (UCS).

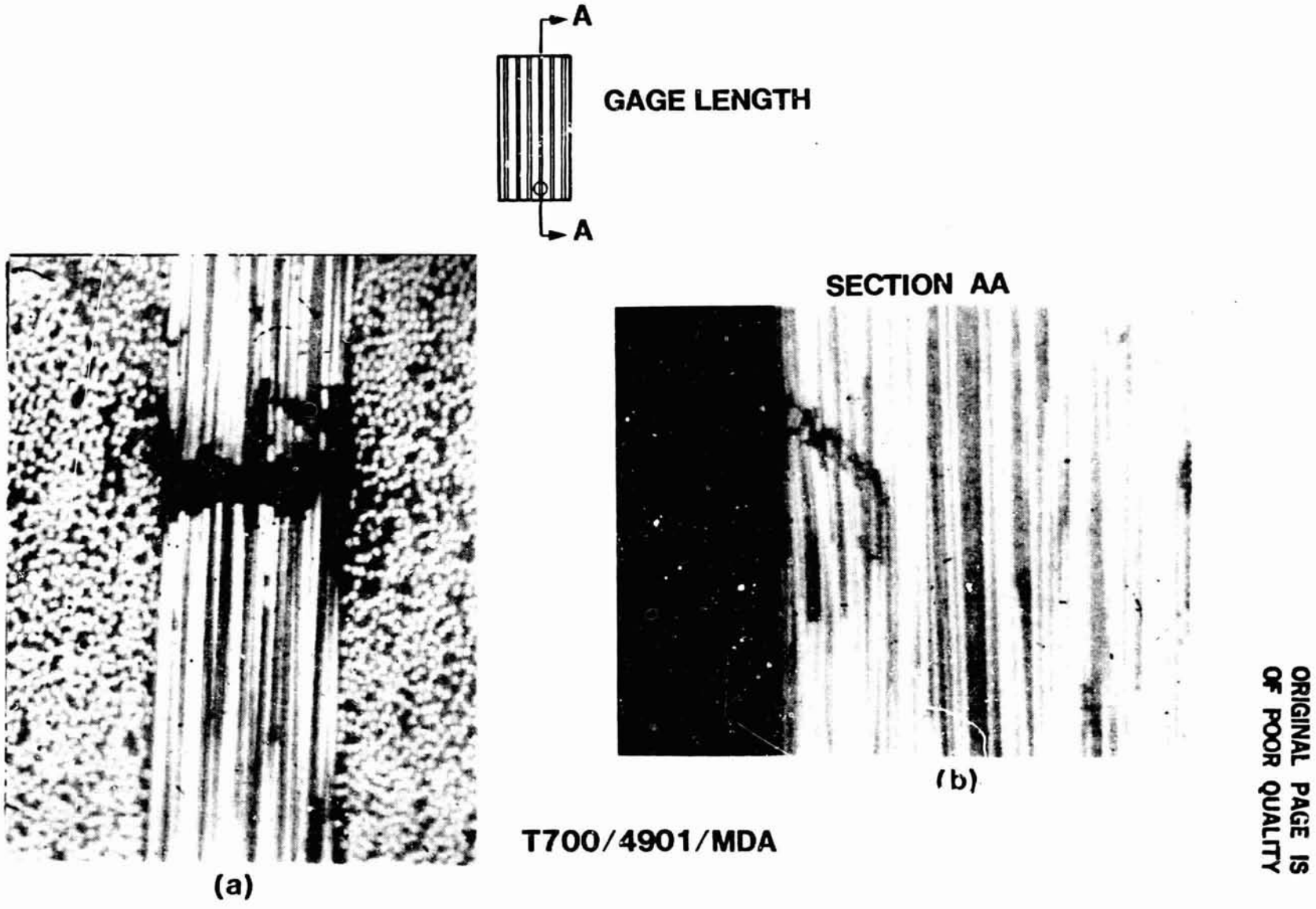

Figure 2. Partial failure in a T700/4901/MDA specimen loaded to 93% of UCS.

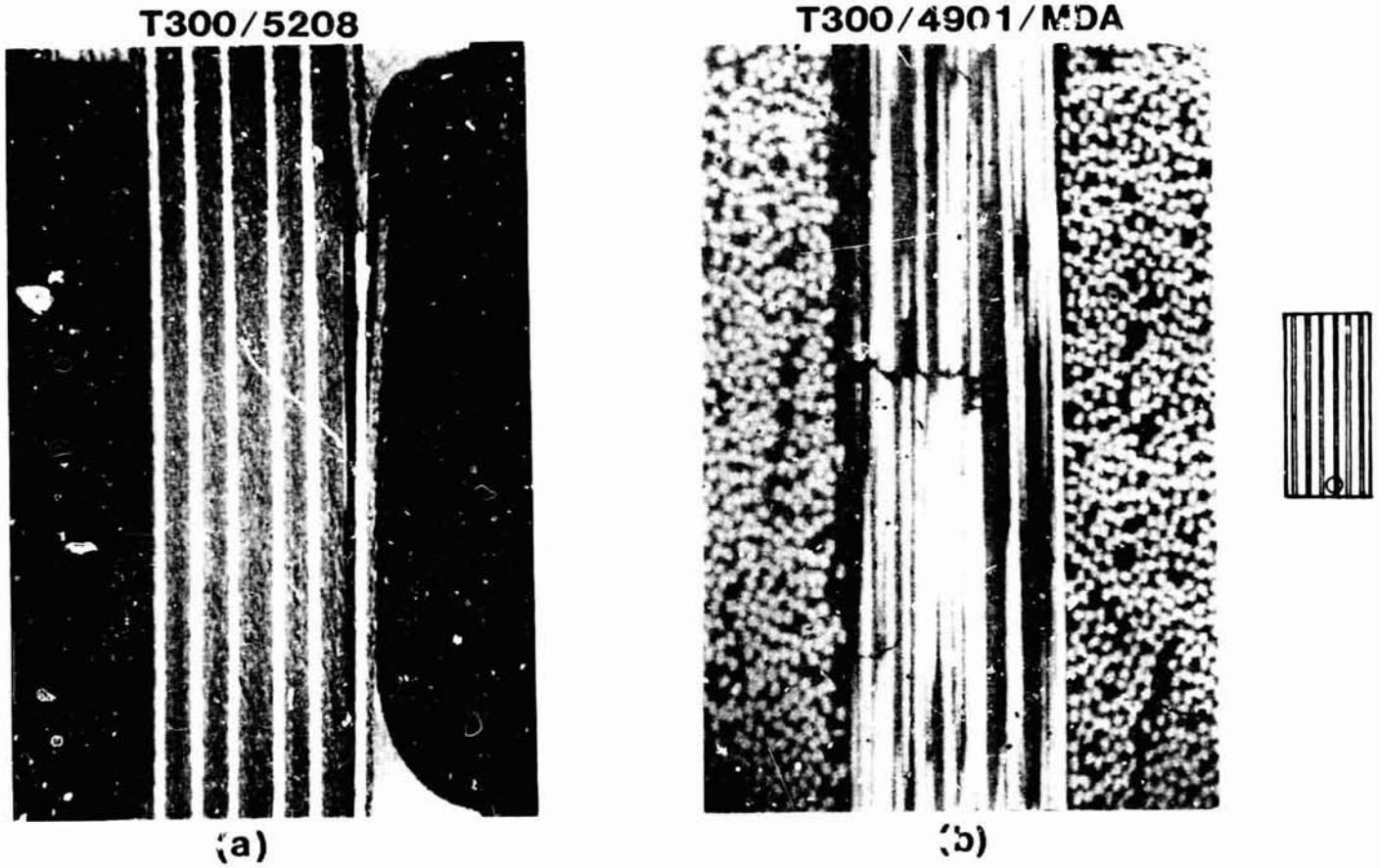

Figure 3. Partial failure in T300/5208 (96% of UCS), T300/4901/MDA (93% of UCS), T300/4901/mPDA (92% of UCS), T700/BP907 (78% of UCS), and T700/4901/mPDA (98% of UCS) specimens.

Figure 3. Continued.

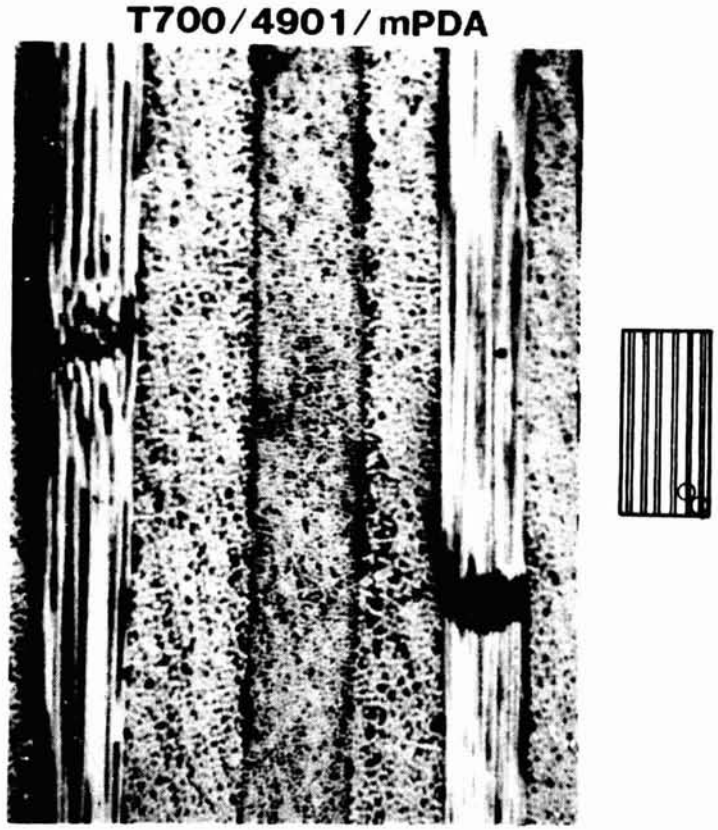

Figure 3. Concluded.

Figure 4. Typical global buckling of sub-laminates following delamination.

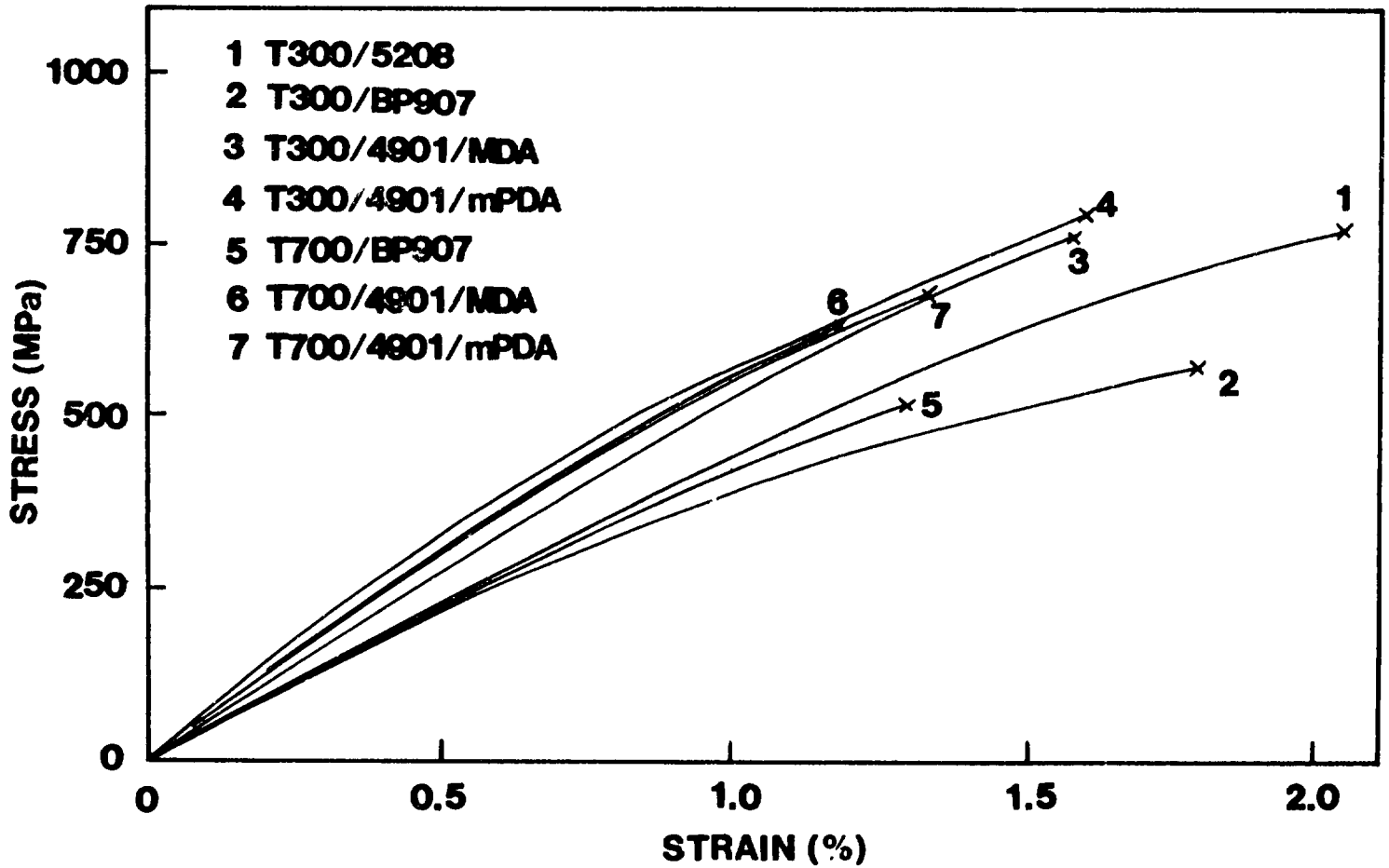

Figure 5. Typical stress-strain curves of different laminates.

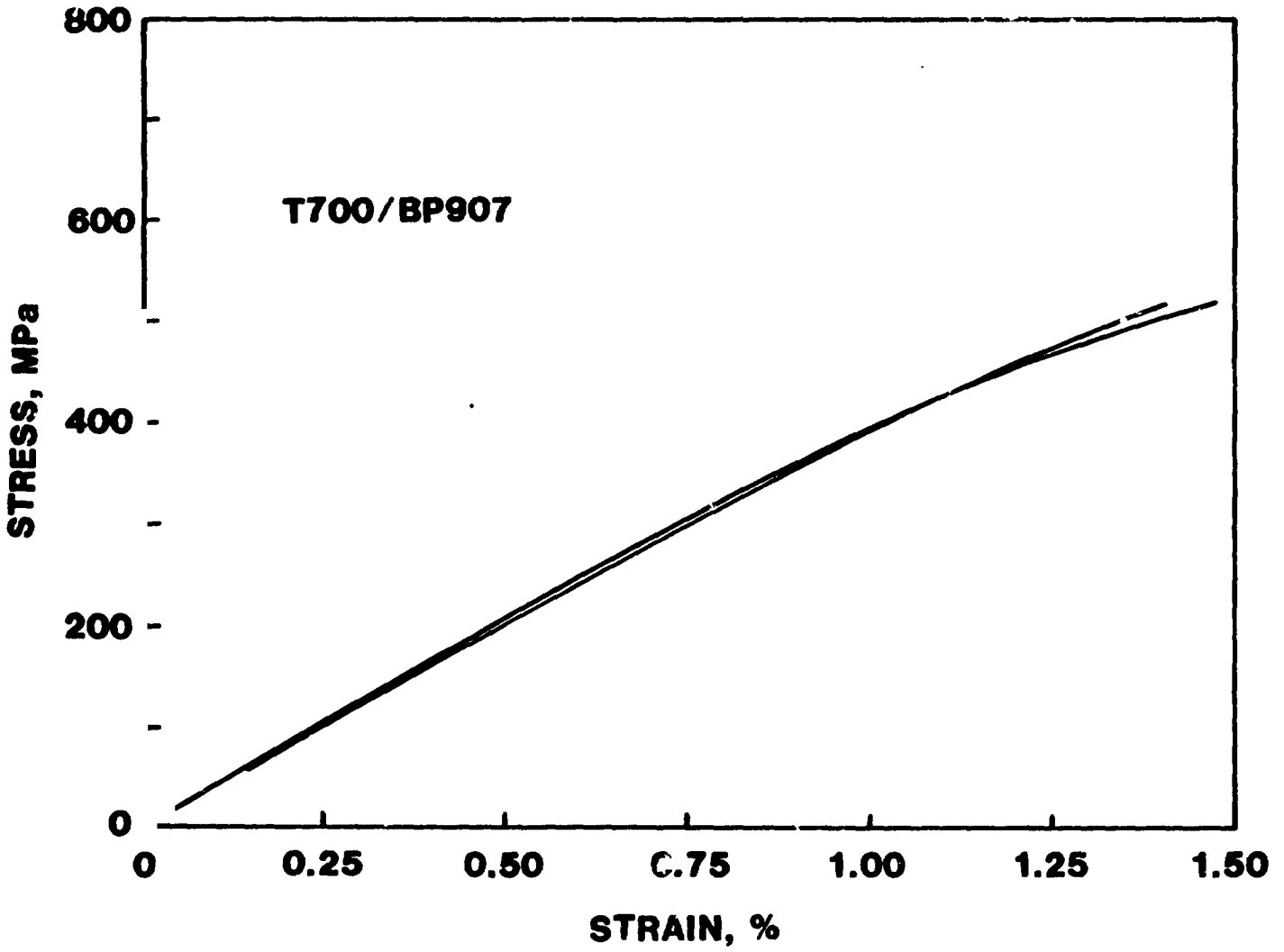

Figure 6. Stress-strain curves for a T700/BP907 specimen with back o-back strain gages

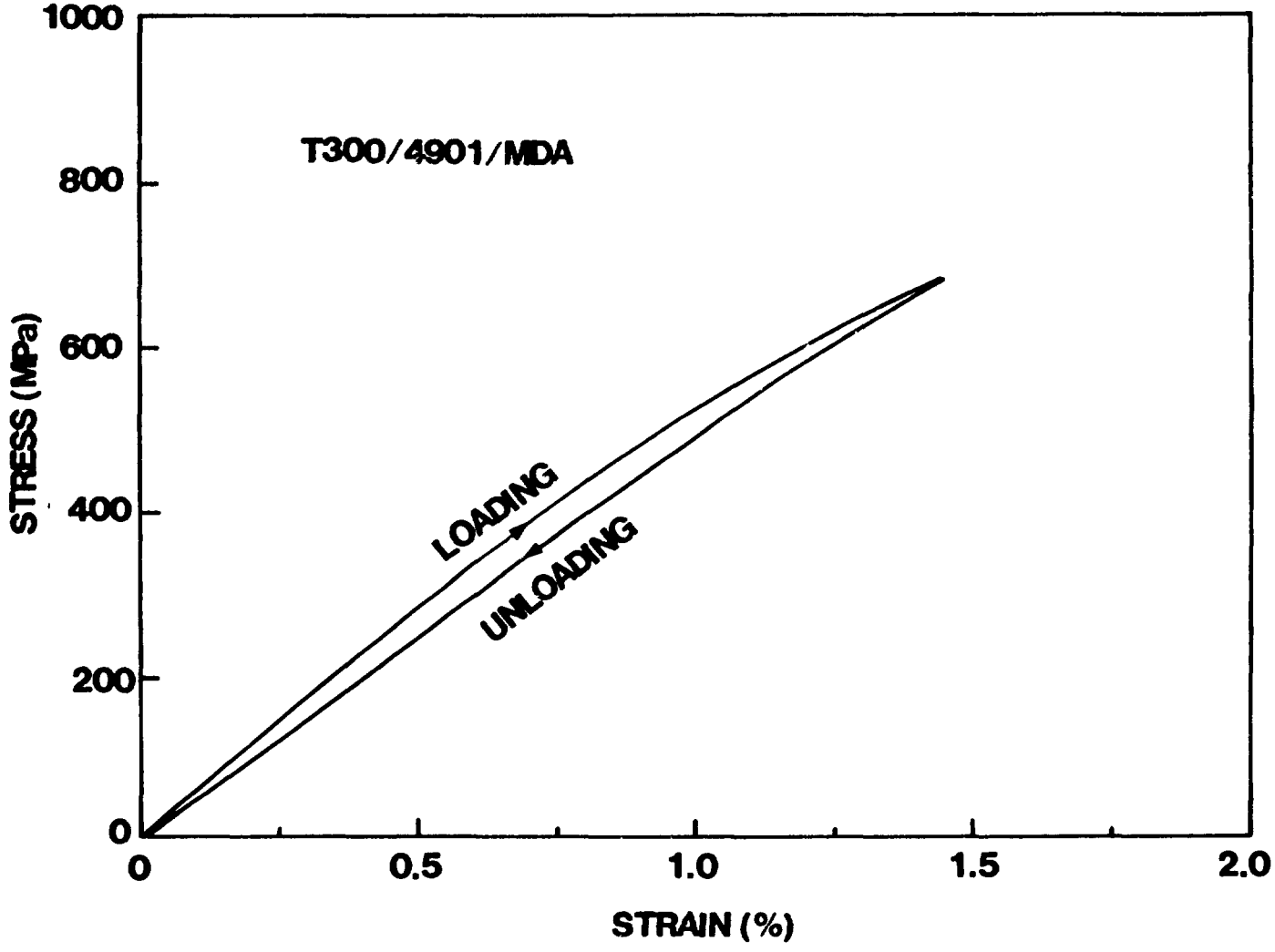

Figure 7. Loading-unloading stress-strain curves for a T300/490/MDA specimen.

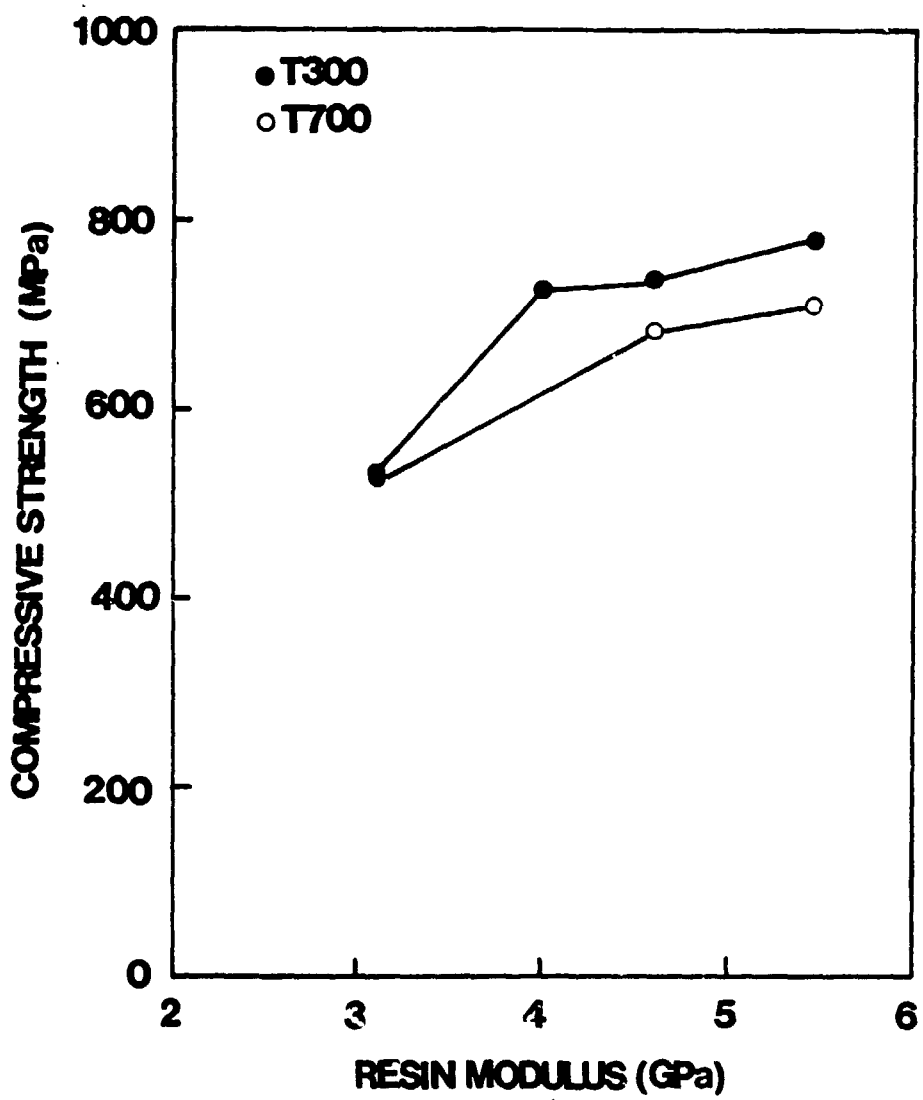

Figure 8. Effect of resin tensile modulus on compressive strength of quasi-isotropic laminates.

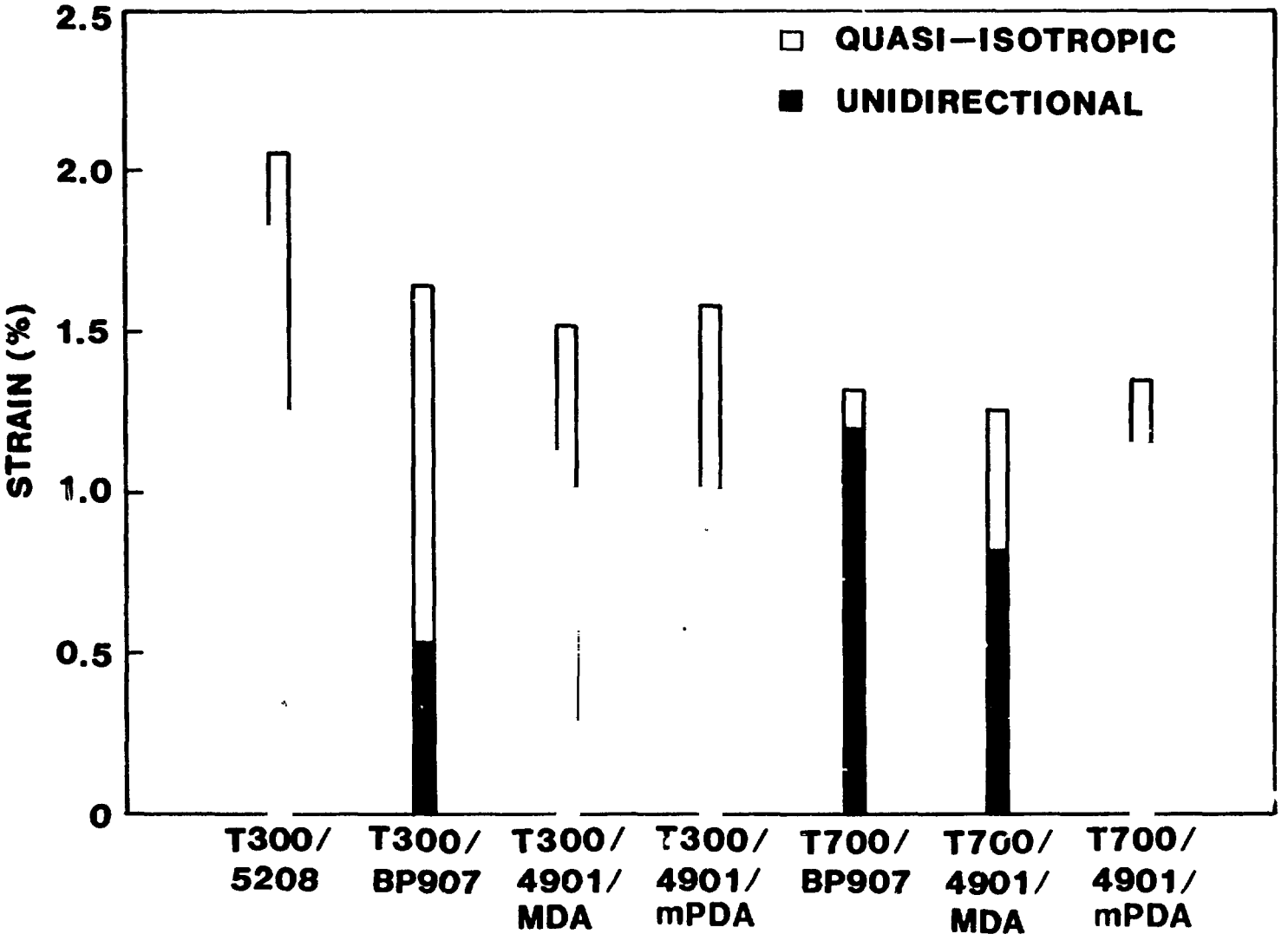

Figure 9. Comparison in failure strain between quasi-isotropic laminates and unidirectional laminates of the same material systems.

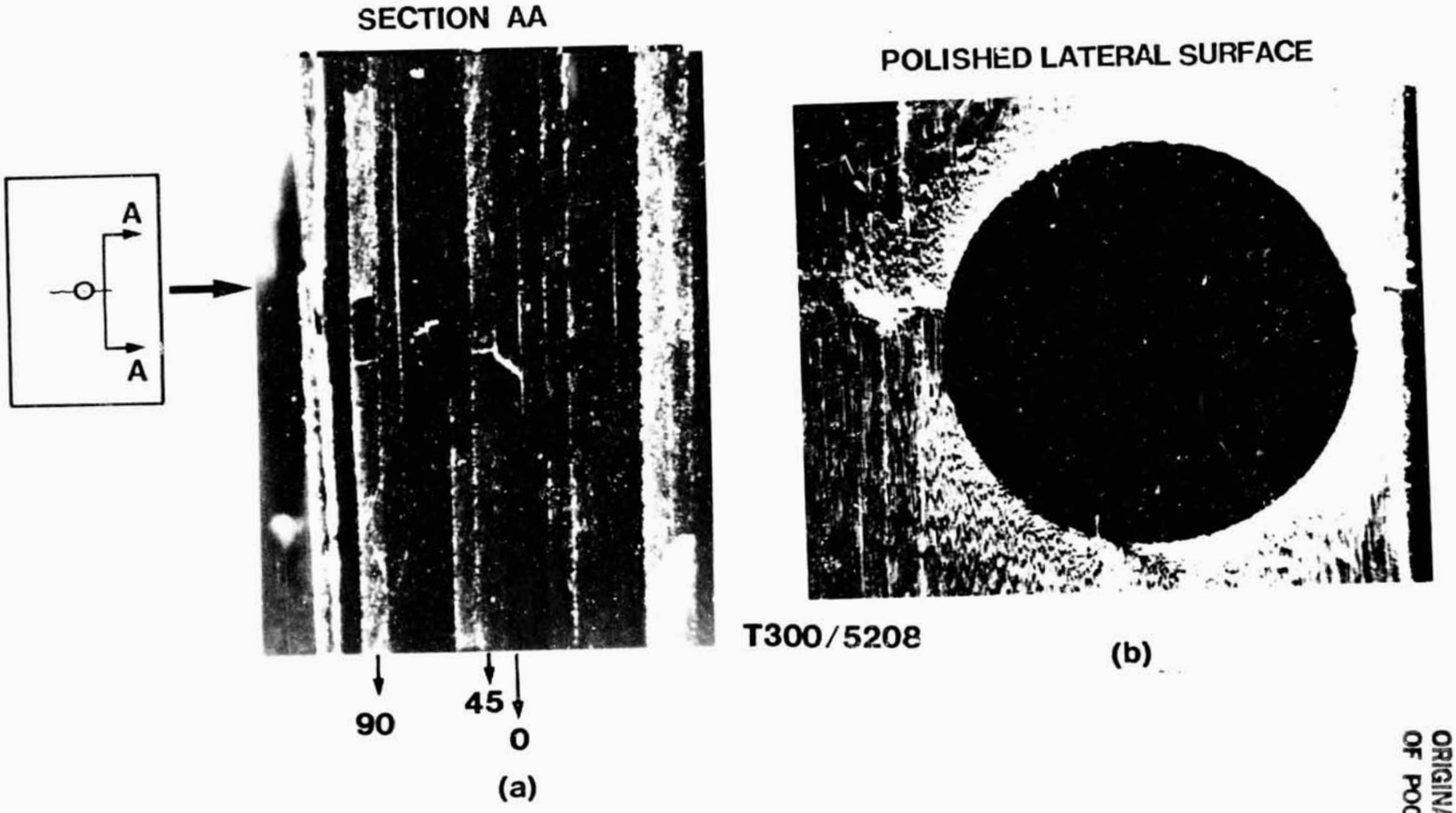

Figure 10. Partial failure in a notched T300/5208 specimen: d/w = 0.125.

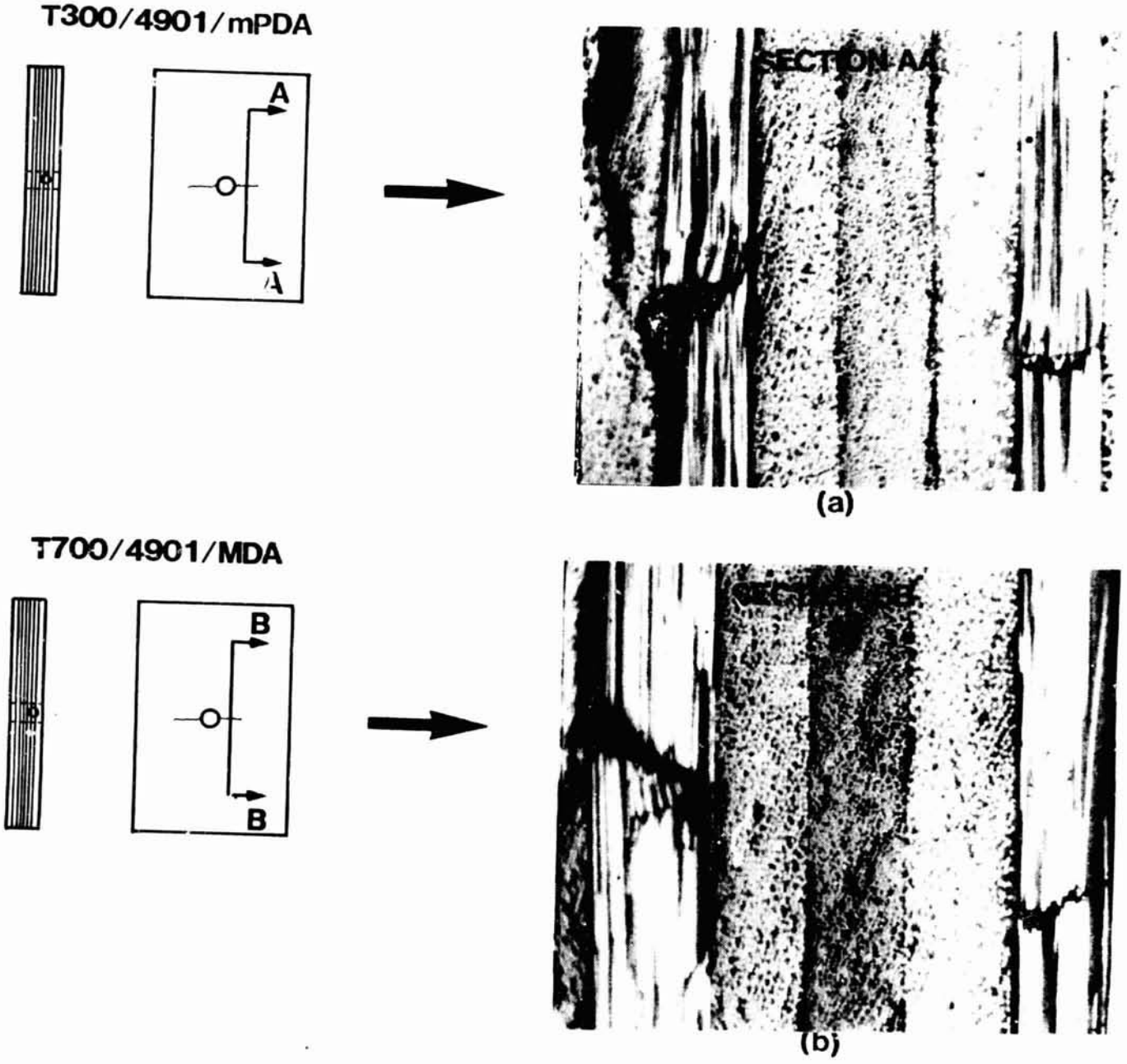

Figure 11. Partial failures in notched T300/4901/mPDA and T700/4901/MDA specimens; d/w = 0.125.

Figure 12. Partial failure in a notched T700/BP907 specimen; d/w = 0.250.

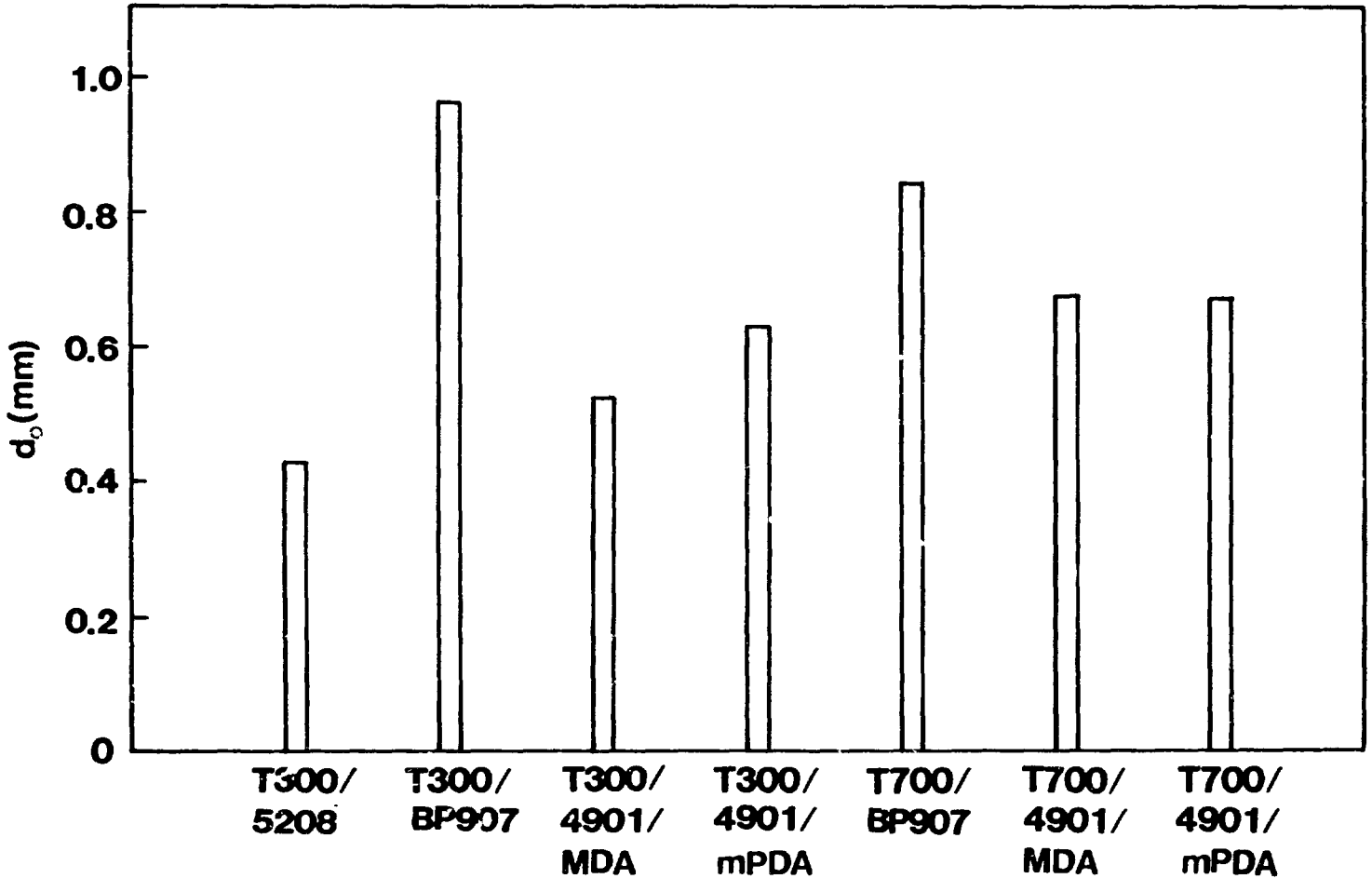

Figure 13. Average values of characteristic length d_o for different laminates.

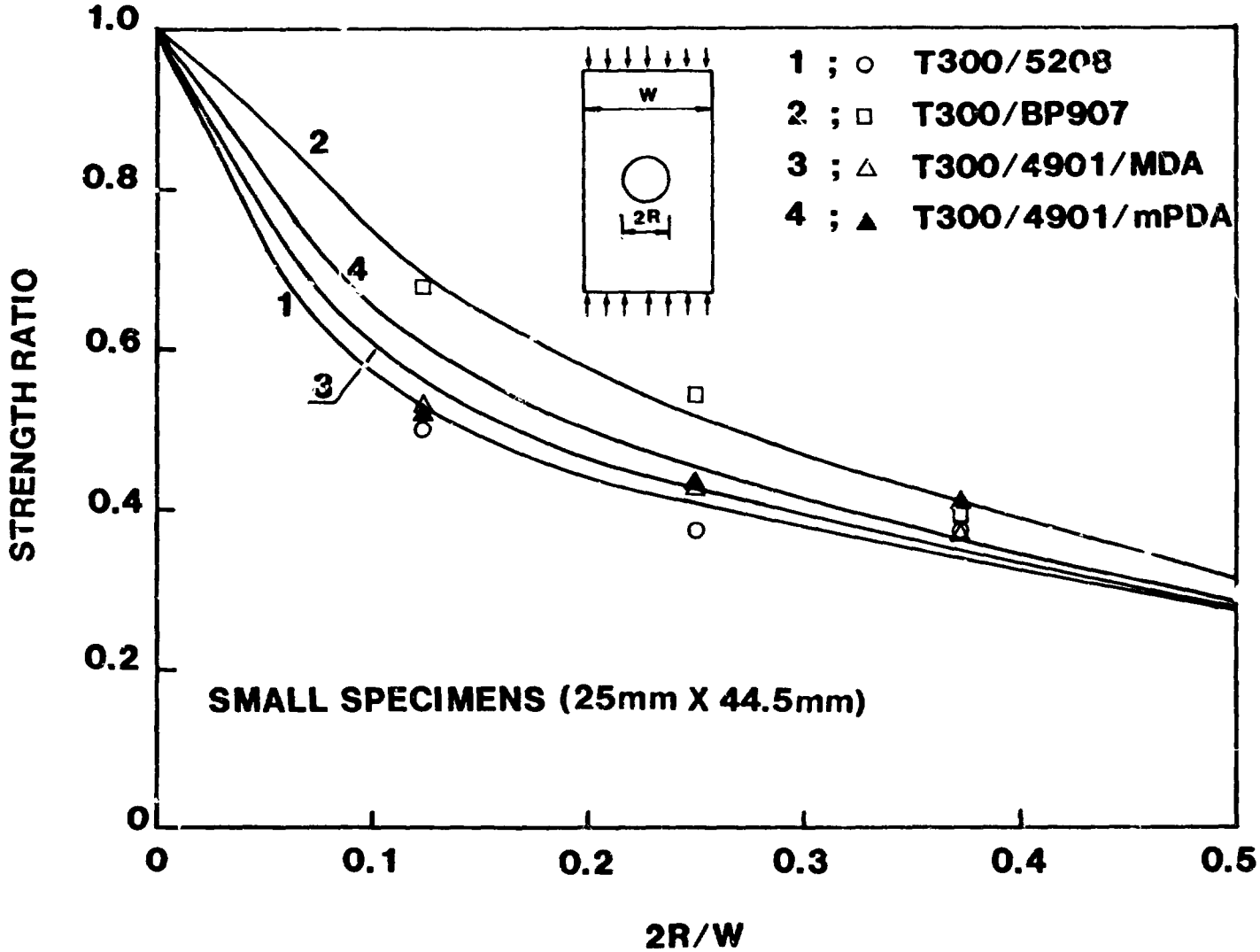

Figure 14. Change of unnotched-to-notched strength ratio with normalized hole diameter: T300 laminates 25 mm wide by 44.5 mm long.

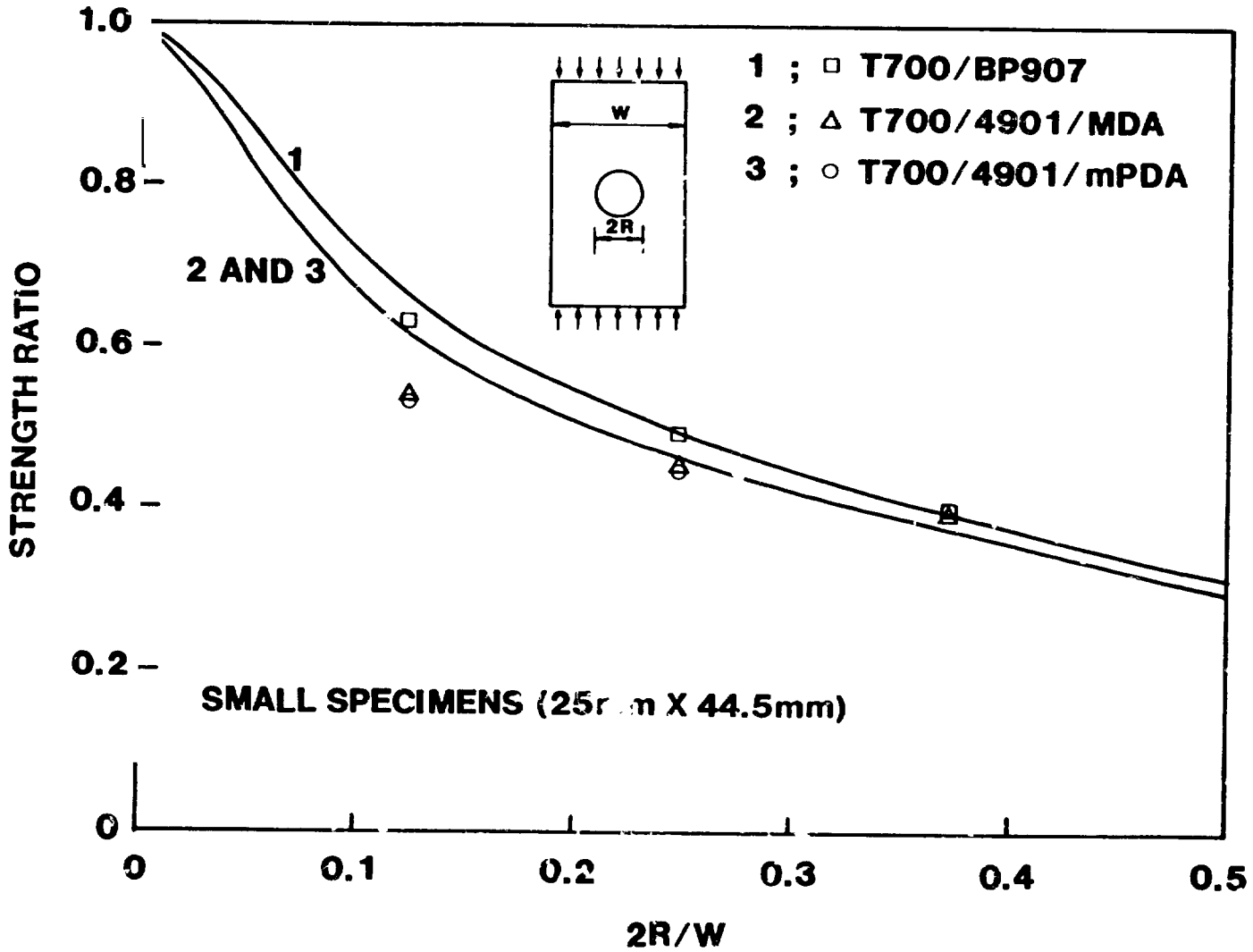

Figure 15. Change of unnotched-to-notched strength ratio with normalized hole diameter: T700 laminates 25 mm wide by 44.5 mm long.

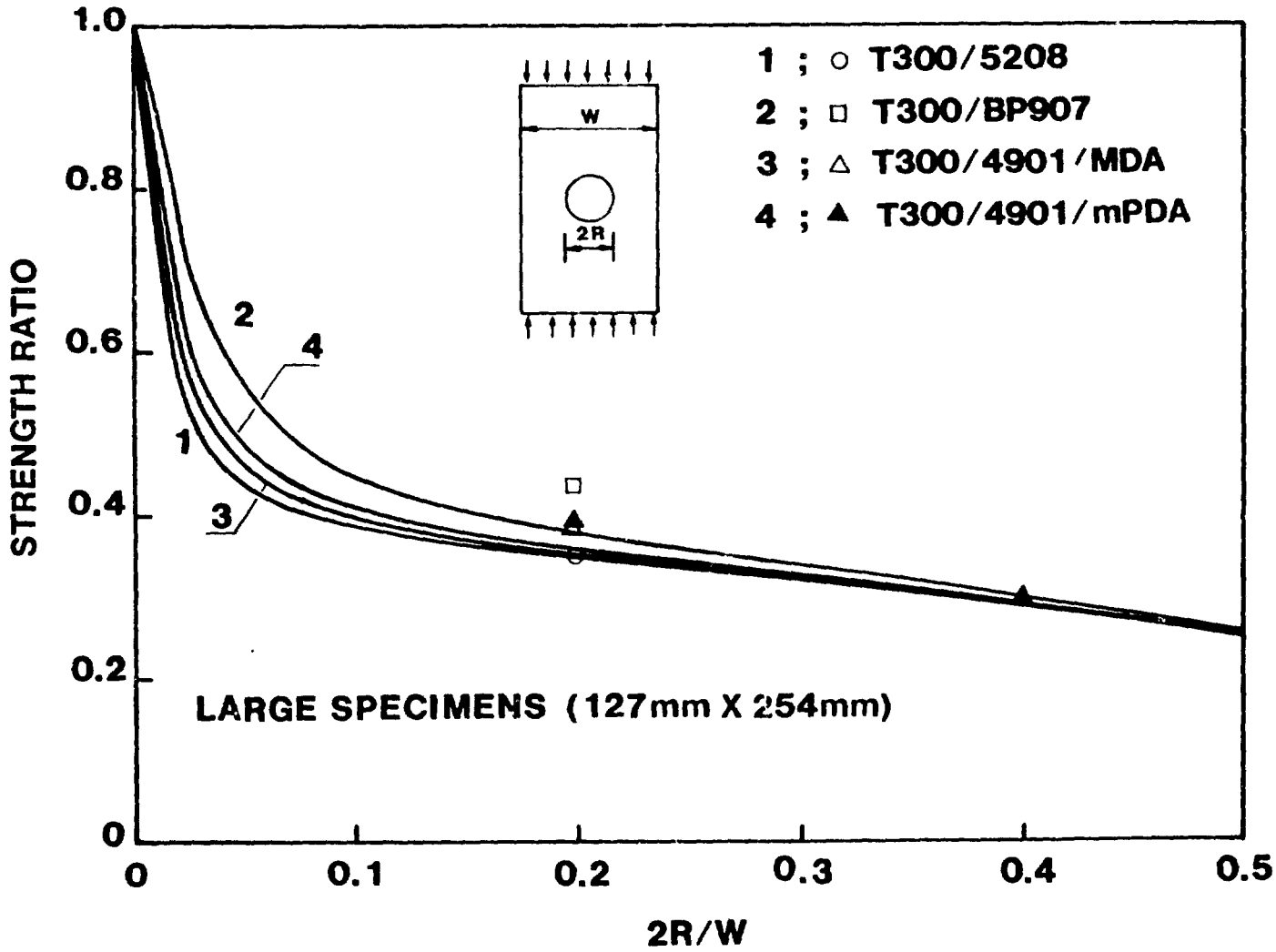

Figure 16. Change of unnotched-to-notched strength ratio with normalized hole diameter: T300 laminates 127 mm wide by 254 mm long.

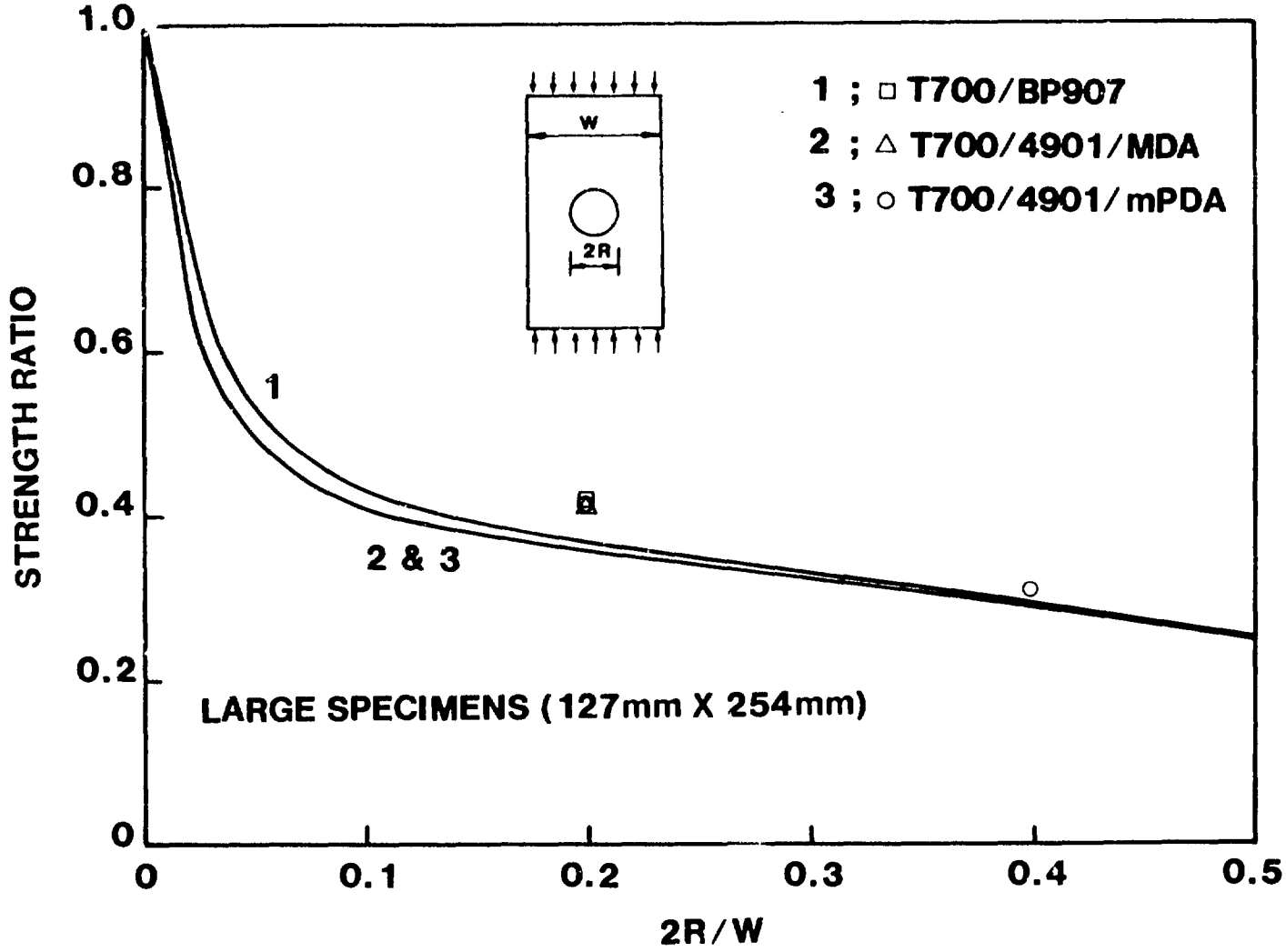

Figure 17. Change of unnotched-to-notched strength ratio with normalized hole diameter: T700 laminates 127 mm wide by 254 mm long.

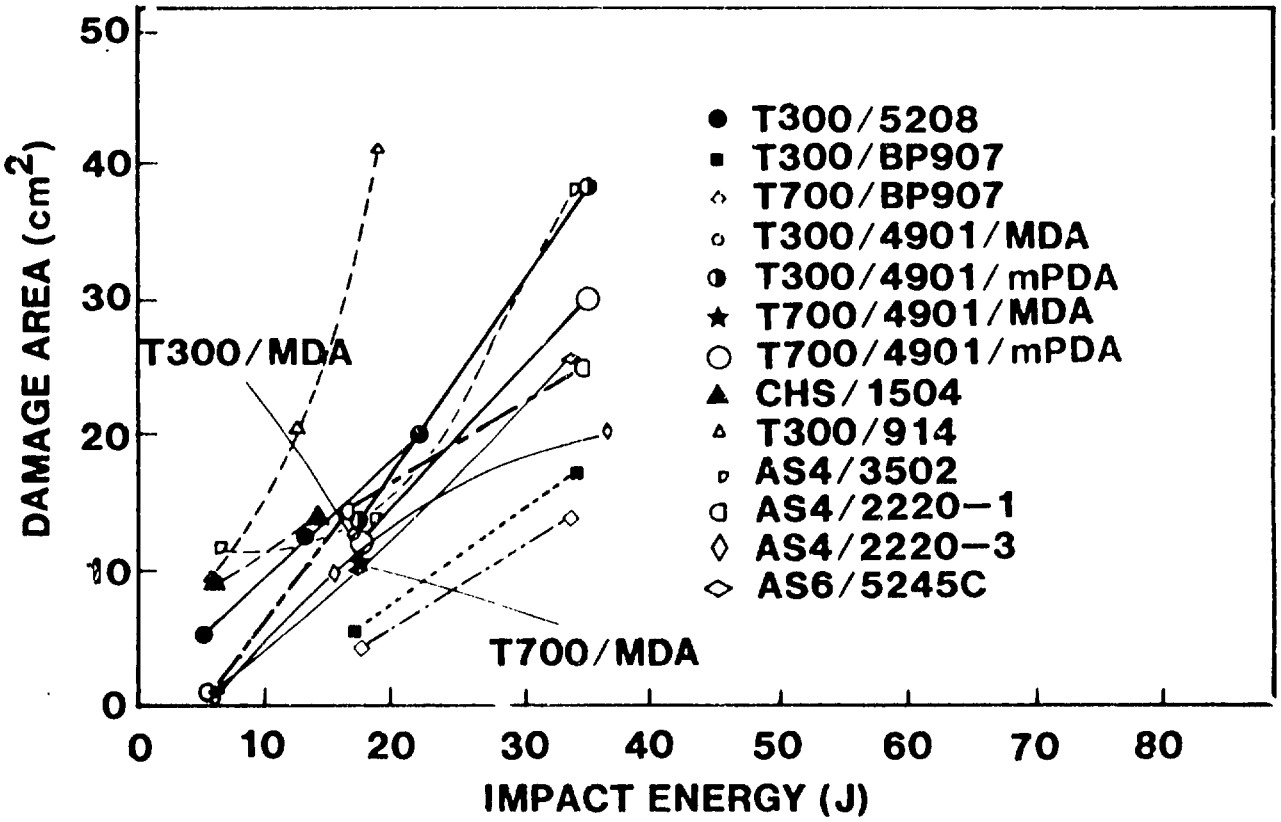

Figure 18. Effect of impact energy on damage area.

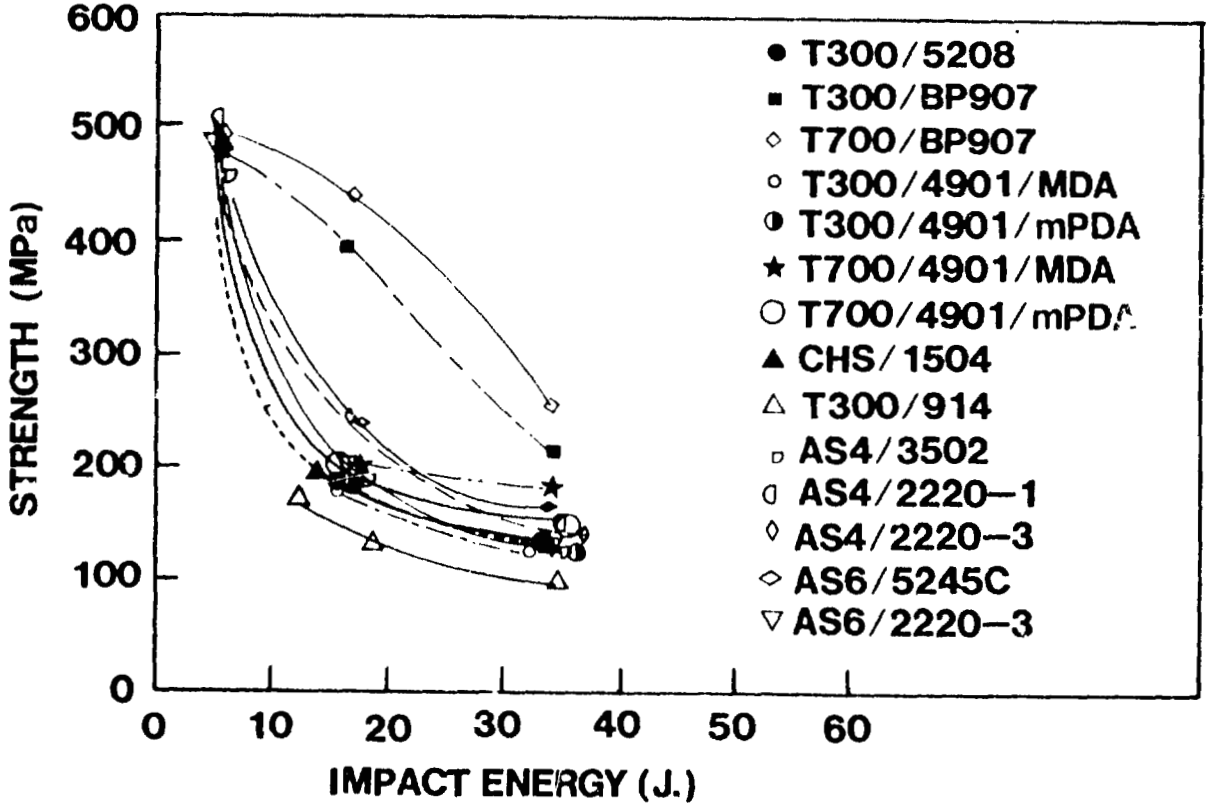

Figure 19. Effect of impact energy on compressive strength.

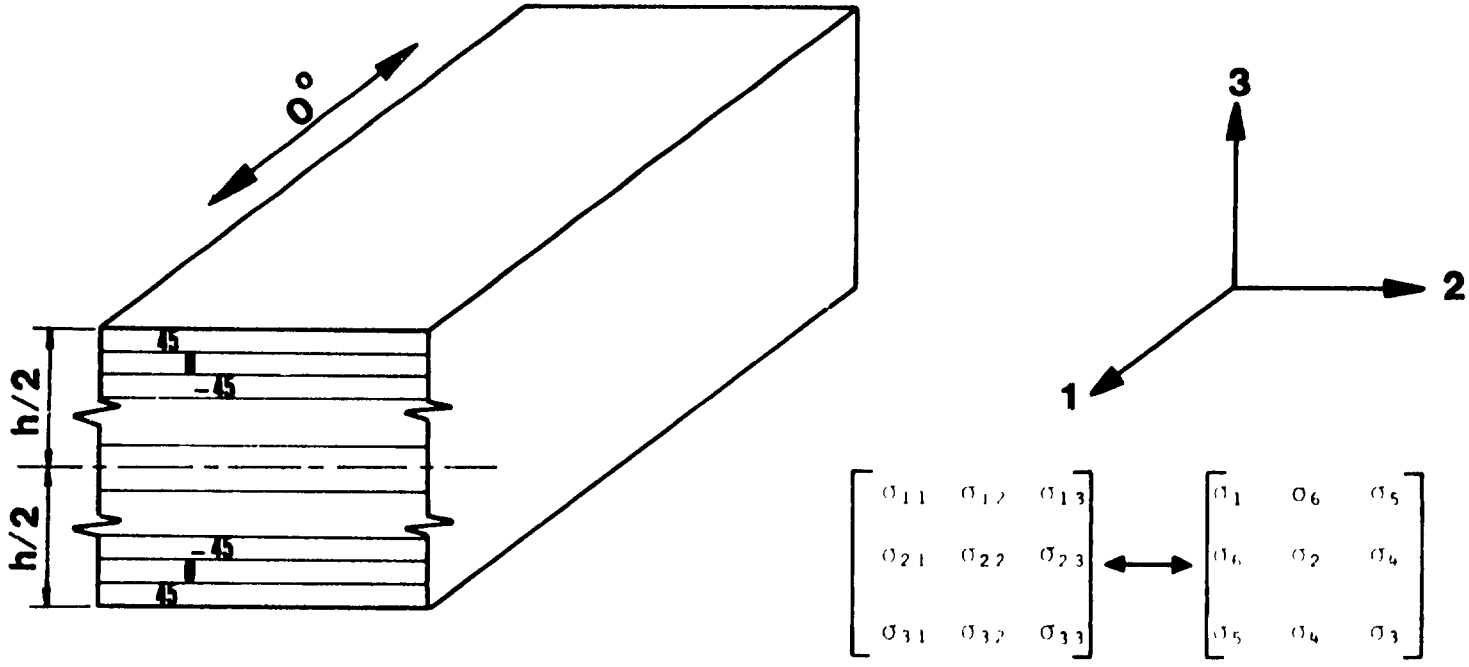

Figure 20. Coordinate axes and the stress notation used in the appendix.

Standard Bibliographic Page

1. Report No.	2. Government Accession No.	3. Recipient's Catalog No.
NASA TM-87604		

4. Title and Subtitle	5. Report Date
The Effect of Resin Toughness and Modulus on Compressive Failure Modes of Quasi-Isotropic Graphite/Epoxy Laminates	March 1986
	6. Performing Organization Code 534-06-23-08
7. Author(s)	8. Performing Organization Report No.
Mohsen M. Sohi, H. Thomas Hahn, and Jerry G. Williams	
9. Performing Organization Name and Address	10. Work Unit No.
NASA Langley Research Center Hampton, VA 23665-5225	11. Contract or Grant No.
12. Sponsoring Agency Name and Address	13. Type of Report and Period Covered
National Aeronautics and Space Administration Washington, DC 20546	Technical Memorandum
	14. Sponsoring Agency Code

15. Supplementary Notes

H. Thomas Hahn is a Professor and Mohsen M. Sohi a student at Washington University in St. Louis, Missouri.

16. Abstract

Compressive failure mechanisms in quasi-isotropic graphite/epoxy laminates were characterized for both unnotched and notched specimens and also following damage by impact. Two types of fibers (Thornel 300 and 700) and four resin systems (Narmco 5208, American Cyanamid BP907, and Union Carbide 4901/MDA and 4901/mPDA) were studied. For all material combinations, failure of unnotched specimens was initiated by kinking of fibers in the 0-degree plies. A major difference was observed, however, in the mode of failure propagation after the 0-degree ply failure. The strength of quasi-isotropic laminates in general increased with increasing resin tensile modulus. The laminates made with Thornel 700 fibers exhibited slightly lower compressive strengths than did the laminates made with Thornel 300 fibers. The notch sensitivity as measured by the hole strength was lowest for the BP907 resin and highest for the 5208 resin. For the materials studied, however, the type of fiber had no effect on the notch sensitivity. The area of impact damage was smallest for the BP907 resin. The 4901 resins were comparable to the 5208 resin in their impact resistance. Of the two fiber types, the T700 fiber consistently gave smaller damage area. The strength reduction after impact could be explained from the impact damage area and the unnotched strength.

17. Key Words (Suggested by Authors(s))	18. Distribution Statement
graphite/epoxy composites quasi-isotropic laminates compressive failure fiber kinking delamination resin modulus notch sensitivity impact damage	Unclassified - Unlimited Subject Category 24

19. Security Classif.(of this report)	20. Security Classif.(of this page)	21. No. of Pages	22. Price
Unclassified	Unclassified	46	A03

For sale by the National Technical Information Service, Springfield, Virginia 22161